Heliyon 8 (2022) e09112

Contents lists available at ScienceDirect

Heliyon

journal homepage: www.cell.com/heliyon

Research article

Synthesis of clay-biochar composite for glyphosate removal from aqueous solution

Danga Rallet [a], Abba Paltahe [b,*], Cornelius Tsamo [b,c], Benoît Loura [d]

[a] Department of Chemistry, Faculty of Sciences, University of Maroua, P. O. Box 814, Maroua, Cameroon
[b] Department of Chemistry, Higher Teachers' Training College, University of Maroua, P. O. Box 55, Maroua, Cameroon
[c] Department of Agricultural and Environmental Engineering, College of Technology, University of Bamenda, Bambili, Cameroon
[d] Department of Textile and Leather Engineering, National Advanced School of Engineering, University of Maroua, P.O. Box: 46, Maroua, Cameroon

ARTICLE INFO

Keywords:
Adsorption
Biochar
Composite
Glyphosate
Wastewater

ABSTRACT

In this work, Clay-Biochar composite was synthesized from local Clay and local cotton wood, and applied for removal of glyphosate from aqueous solutions by adsorption. The Clay, Biochar and Clay-Biochar composite were characterized using X-ray diffraction, scanning electron microscope, fourier transform infrared spectroscopy, and thermal analysis. The adsorption studies of glyphosate were investigated by batch process at laboratory temperature. Adsorption experiments showed that the composite exhibited much better adsorption capability than both Clay and Biochar. The adsorption kinetics of glyphosate obeyed pseudo-second-order model according to their high coefficient R^2 = 0.996, 0.995, 0.999 for Clay, Biochar and Clay-Biochar composite, respectively. The equilibrium adsorption data was best described by Langmuir model with R^2 values of 0.937, 0.989, and 0.993 and Temkin model with R^2 values of 0.982, 0.909, and 0.983, each for Clay, Biochar and Clay-Biochar respectively. Therefore, Clay-Biochar composite could be applied in the remediation of glyphosate in contaminated aqueous media.

1. Introduction

It is generally said that water is life. Unfortunately, it is the main victim of environmental pollution. The reduction in the quality of physico-chemical and biological characteristics of water due to environmental pollution is referred to as water pollution. Human activities are largely responsible for the presence of xenobiotic compounds in water bodies as pollutants because their concentrations exceed the natural levels. Two major sources; increased urbanization as well as increased industrial activities are responsible for the increase in the pollution of water bodies by xenobiotic compounds. Some examples of these xenobiotic compounds being sent to the environment at large include pesticides, dye, heavy metals etc. [1].

The particular group of xenobiotic called pesticides has been used and continues to be used for insects, weeds and diseases management in agricultural activities. Their improper use can lead to serious consequences on non-target organisms through different routes of exposures which can be direct and indirect. 65 % of the pesticide market (herbicides, insecticides, and fungicides) worldwide is dominated by herbicide. One example of herbicide generally used in agriculture, industrial and urban activities is glyphosate (N-(phosphonomethyl)-glycine). This wide domain of usage is because it is a post-emergence herbicide having a broad spectrum and non-selective. Currently, annual usage of glyphosate worldwide stands at about 600–750 thousand tonnes and is expected to increase to 740 to 920 thousand tonnes by 2025 [2,3]. The World Health Organization (WHO) has reported teratogenicity effect of glyphosate compounds in vertebrates. This has resulted in glyphosate being classified as a probable human carcinogen by WHO. Metabolic acidosis has been reported as the main clinical symptom from glyphosate contamination in humans which occurs through accidents, or labor intoxication and its metabolites [4, 5]. Due to glyphosate toxicity, there is an urgent need to eliminate it from wastewater as water is used for every activity on earth. Most conventional methods currently used to eliminate glyphosate from water and wastewater include; chemical oxidation, electrolysis, biochemical, adsorption and evaporation. However, recent studies worldwide show an evolving trend in the use of adsorption because of its ability to be operated at low cost with almost no energy consumption. Adsorption also has the potential to eliminate all types of pollutants at every concentration [6]. Of particular importance is the use of local materials and wastes as adsorbent in adsorption.

* Corresponding author.
E-mail address: abbapaltahe@yahoo.fr (A. Paltahe).

https://doi.org/10.1016/j.heliyon.2022.e09112
Received 27 December 2021; Received in revised form 31 January 2022; Accepted 10 March 2022

Clay is one of the most abundant natural materials worldwide. While clay has a wide range of application with its use as adsorbent included, each application is highly depended on its physical and chemical properties defined by structure and composition [7]. Different types of clays are characterized by high surface areas, many surface hydroxyl and silanol groups, high cationic exchange capacity and are chemically and mechanically stable [8, 9]. These characteristics give them good adsorbent potentials. However, these adsorbent properties can be improved by combining the clay with other materials. In this light, bentonite based composites have been synthesized between bentonite and; metal oxide, synthetic and natural polymers. Equally other authors have also reported the potential of synthesizing clay composites using biochar from biomass waste [7].

Biochar (BC) produced by pyrolysis of biomass in the absence or limited oxygen condition is actually a charcoal rich in carbon [8, 9]. Biochar can be used for many applications amongst which environmental remediation [10, 11, 12]. This is because it has a negative surface charge, many surface functional groups, and other structural and textural properties such as high specific surface area, large pore volume, and high cationic exchange capacity. These properties thus give biochar a strong binding capacity for organic and inorganic pollutants [13, 14, 15]. The chemical and physical properties of biochar are influenced by feedstock types which are abundant and easily available as waste materials. Temperature, residence time, heating rate, and reactor type are some of the conditions that influence biochar pyrolysis process [11, 16]. The use of biomass as feedstock for biochar production supports sustainable waste management indirectly. A number of researchers have recently attempted to synthesize biochar composites to improve its properties and increase domains of applications [17]. Because clay and biomass (precursor for biochar) are easily available materials worldwide, the use of these two materials to produce a composite with good adsorbent properties for environmental remediation particularly water treatment will provide a cost effective process and reduce environmental effects of biomass dumping [7].

Many studies have synthesized clay-biochar composites and used it to remove several pollutants such as methylene blue, ammonium, cadmium, tetracycline antibiotic, arsenic and nitrate from aqueous media [7, 8, 17, 18, 19]. However, there is no article reported on the adsorption of glyphosate by clay-biochar composite to the best of our knowledge.

In the present study, the clay-biochar composite was produced from local cotton wood and local clay and the efficiency of the produced composite, raw clay and cotton wood biochar materials in removing glyphosate from synthetic wastewater through batch experiments was evaluated. The adsorbent properties of these materials were also determined.

2. Material and methods

2.1. Adsorbents preparation

2.1.1. Sample and treatment of clay

The clay sample was obtained from the far north region of Cameroon, in the area of Maroua. The purification of natural clay used in this work was done according to the method described by [20]. Accordingly, clay was washed and rinsed with distilled water to remove stones and other heavy particles, dried at 105 °C in the oven for 12 h. Carbonates were eliminated using hydrochloric acid (0.5 M) solution to obtain the clay particles and the solid was crushed in a porcelain mortar and sieved through a 250-mesh sieve. Clay fractions (<2 μm) were separated by sedimentation.

2.1.2. Biochar production

Cotton woods were collected from a farm in Maroua. Cotton woods were cut into small pieces and washed with distilled water to remove adhered contaminations from its surface. After washing with distilled water, the small pieces of cotton woods were dried at 80 °C in the oven for 12 h. Before pyrolysis, the small pieces of wood were milled into little particles. Biochar was produced by the slow pyrolysis from the little particles obtained. The pyrolysis was performed in a quartz tube at a heating rate of 15 °C/min up to 650 °C, the maximum reaction temperature was kept constant for 2 h in order to assure the completion of the reactions.

2.1.3. Clay-biochar composite production

Clay-biochar composite was prepared from clay mineral and cotton wood. First, a stable clay suspension was prepared by adding 10 g of clay powder to 200 mL distilled water and mixed using a rotary shaker for 20 min. Then, 10 g of the milled cotton wood were dipped into the clay suspensions and stirred for 2 h. After that, the mixture was poured in an inox plate and oven dried at 80 °C. The mixture of clay with milled cotton wood was pyrolysed in the same condition as biochar. Then the biochar and composite were washed with deionized water, freeze-dried, passed through a 250-mesh sieve, and used for characterization experiments. The clay, biochar and clay-biochar composite were denoted as CL, BC and CBC composite respectively.

2.2. Adsorption experiments

The adsorption performance was carried out by mixing 0.01 g of adsorbent with 50 mL of glyphosate solution in 250 mL capped Erlenmeyer flask and stirred on a rotary shaker at laboratory temperature up to desired time. For investigation of operational paramters; the influence of contact time was studied for different contact time (5–240 mn), effect of pH was studied for pH of 4, 6, 8, 10 and 12. For isothermal assays the concentrations were varied from 10–100 mg/L pH was adjusted by adding 0.1 M HCl or 0.1 M NaOH. After predetermined intervals, the solution was filtered using Whatman filter paper No 1, and the equilibrium concentration of glyphosate remaining in solution was determined in a UV/visible spectrophotometer (spectrumlab 22) at wavelength 700 nm by complexing as discribed by [21], from the previously determined calibration curve. All the samples were measured in duplicate and the average value was used. The amount of adsorbate of glyphosate adsorbed by different adsorbents was calculated by Eq. (1).

$$q_e = \frac{(C_0 - C_e)}{m} V \tag{1}$$

where q_e (mg g^{-1}) represents the amount of glyphosate adsorbed per gram (g) of adsorbent, C_o and C_e indicate initial and final glyphosate solution concentrations (mg L^{-1}) respectively, m is the mass of adsorbent (g), and V is the volume of solution (L).

2.3. Kinetic models and isotherm adsorption

Kinetic models are essential to determine the rate of adsorption process and to give important information on the reaction mechanism. The Kinetic data was analyzed using: pseudo-first order model (Eq. (2)).

$$\ln(q_e - q_t) = \ln(q_e) - k_1 t \tag{2}$$

and pseudo-second order model (Eq. (3)).

$$\frac{t}{q_t} = \frac{1}{k_2 q_e^2} + \frac{t}{q_e} \tag{3}$$

where q_t and q_e are the amount of adsorbate at any time t and at equilibrium time (mg g^{-1}) respectively, k_1 (min^{-1}) and k_2 (g mg^{-1} min^{-1}) are the pseudo-first order and pseudo-second order equilibrium rate constant that were determined through linear plot of $\ln(q_e - q_t)$ versus t and t/q_t versus t.

Three isothermal models; Langmuir, Freundlich and Temkin were used to fit experimental data. Correspondingly, the following linearized

forms of these models were applied for the adsorption isotherms; Langmuir (Eq. (4)), Freundlich (Eq. (5)) and Temkin (Eq. (6)).

$$\frac{1}{q_e}=\frac{1}{q_m C_e k_L}+\frac{1}{q_m} \tag{4}$$

$$\ln q_e=\ln k_F+\frac{1}{n}\ln C_e \tag{5}$$

$$q_e=b\ln k_T+b\ln C_e \tag{6}$$

where C_e (mg L^{-1}) is the equilibrium concentration of glyphosate solution, q_e and q_m (mg g^{-1}) are the amount adsorbed and maximum adsorption capacity respectively, k_L is the Langmuir constant (L mg^{-1}). k_F ((mg g^{-1})/(mg L^{-1}) ^{n}) is the Freundlich affinity coefficient and n is a measure of adsorption linearity. k_T (L g^{-1}) is the equilibrium binding constant, b (J mol^{-1}) is related to heat of adsorption.

2.4. Characterization techniques

Different techniques were used to characterize clay, biochar and synthesized clay-biochar composite. X-ray diffraction (XRD) study was performed in a diffractometer (Bruker, D8 ADVANCE) with monochromatic CuKa radiation (k = 1.5418 A°) at 40 KV and 40 mA in a range of 4–80° to determine the phases identification. The surface functional groups analysis was done by the FTIR spectrophotometer (Bruker Make, Model: ALPHA-P). The FTIR reflection spectra were recorded in the

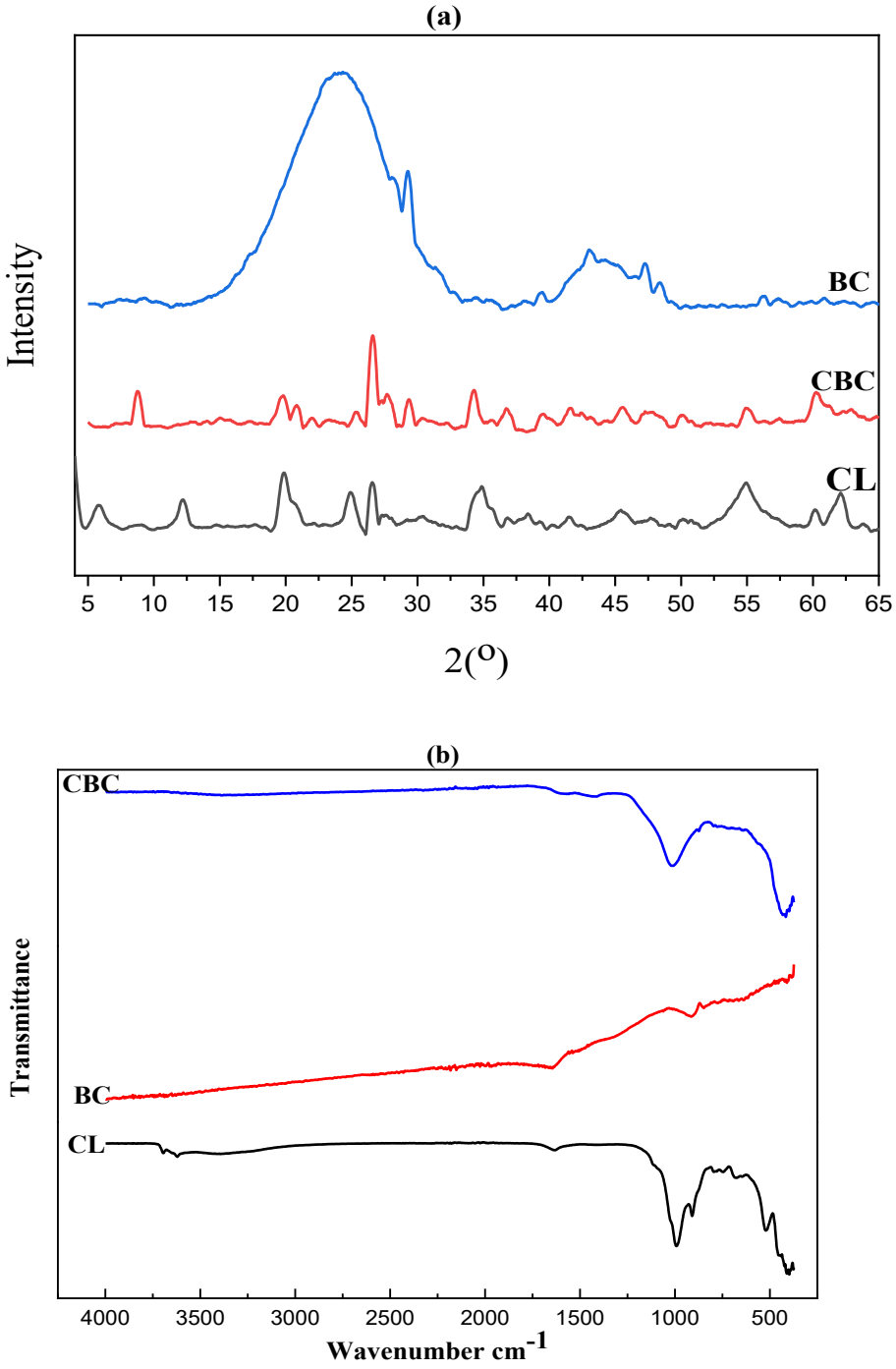

Figure 1. (a) X-ray diffractograms, (b) FTIR spectra of CL, BC and CBC.

region from 400 to 4000 cm^{-1}. Powders of the raw materials (cotton wood and clay) were subjected to thermal analyses (TG and DTA) using a NETZSCH STA 429 (CD) device from 20 to 1200 °C in a self-generated atmosphere of air at heating rate of 5 °C/Min. The morphology and chemical composition of the adsorbents were determined using SEM and EDX analysis respectively. All the different results from the different techniques of characterization were compared with those of similar samples reported in literature for identification.

3. Results and discussion

3.1. Characterization of adsorbents

3.1.1. X-ray diffraction

XRD patterns of Clay, Biochar and Composite are presented in Figure 1a. The XRD diffractogram of clay (CL) revealed diffraction peaks at 2θ = 5.77; 12.21; 19.82; 20.74; 24.88; 26.57; 34.81; 41.59; 45.32; 50; 54.8; 60.23 and 62.13. The price of 2θ for montmorillonite mineral was 5.77; 19.82; 34.81 and 62.13 [22]. The reflections observed at 12.21; 24.88; 41.59 indicate the presence of kaolinite [23, 24]. The other peaks are impurities corresponding to quartz. According to studies of [25, 26] the clay used is a mixture of montmorillonite (type2/1) and kaolinite (type1/1). The XRD analysis of the BC (Figure 1a) mainly exhibited two broad peaks centered at 2θ = 24° and 43° related with the strong and weak diffraction peaks respectively. These peaks indicated the presence of graphite in the biochar. The weak peaks at 43° suggested the amorphous nature of carbons. Similar diffraction patterns were obtained by [27]. As given in Figure 1a, XRD pattern of CBC showed primary reflection at 8.77 which is completely absent in both CL and BC. Meanwhile, the peaks at 5.77 and 12.21 from CL disappeared and there is a significant decrease of the intensity of the peak at 19.82. Quartz (SiO_2), was also found in clay–biochar composite as a common mineral within clay. The changes in the result of CBC show that the production method used successfully implanted biochar onto the clay matrix.

3.1.2. Infrared spectroscopy

The obtained FT-IR spectrums of clay, Biochar and composite are shown in Figure 1b. The FT-IR spectrum of CL revealed bands at 3695, 3621 cm^{-1} which can be assigned to the stretching vibrations of inner and internal hydroxyl groups [23]. The band at 1633 cm^{-1} is attributed to deformation vibration of absorbed water at the interlayer of clay [25]. The bands at 991 cm^{-1} and 793 cm^{-1} are assigned to Si–O stretching vibration of orthosilicates and quartz respectively [28]. The band at 911 cm^{-1} is due to the Al–OH–Al bending vibration. The FTIR bands at 680 and 519 cm^{-1} were attributed to stretching of Si–O–Al bonds (kaolinite and smectite) [23, 25, 29]. The bands around 1646 and 1498 cm^{-1} were attributed to the stretching vibrations of C=O and C=C, corresponding to carbonyls and aromatic rings, respectively in the case of BC [16, 30]. The functional groups appearing at 1181 and 913 cm^{-1} can be assigned to alcoholic C–O stretching and to aromatic C–H bending vibration [13, 30]. Comparing with the results of the raw materials, the composite exhibited bands at 1597, 1442, 1018, 875; 421 cm^{-1}, assigned to C=O and C=C, Si–O–Si, Al–OH–Al, Si–O–Al respectively, which were practically the same functional groups detected in CL and BC with low intensities.

3.1.3. Thermal analysis

Thermal analysis (TG, DTG and DSC) was carried out on the raw clay and the cotton wood as shown in Figure 2. The weight loss during thermogravimetric decomposition was divided into four stages for both raw materials. The raw clay and the cotton wood exhibited a total weight loss of about 31% and 71% up to 1000 °C respectively. In the Figure 2a (TG, DTG and DSC for raw clay), the first weight loss (10.68%) have evidenced between 0 °C–200 °C was due to dehydratation of free water contained in the clay and related to the first endothermic peak at 81 °C. The second weight loss occurred between 250 – 400 °C expressed by an exothermic peak around 348 °C, corresponding to the decomposition of organic matter contained in the clay. The third weight loss (7.74%) observed in the range of 400–600 °C which was revealed by an endothermic peak at 494 °C could be associated with the dehydroxylation of both kaolinite and montmorillonite present in the clay. The last weight loss (1.26%) occurring within the temperature range of 780–950 °C was attributed to dehydroxylation of kaolinite which is transformed into metakaolinite [23, 29]. As shown in Figure 2b, the TG, DTG and DSC curves of cotton wood exhibited four stages weight loss observed in the range within 0 °C–150 °C, 200 °C–360 °C, 360 °C–430 °C and 430 °C–900 °C which were expressed by an endothermic 65 °C, exothermic 295 °C, exothermic 419 °C and exothermic 444 °C respectively. The first stage weight loss of 9.03% was associated with to the loss of water. The second loss of 43.36% could be attributed to the degradation of hemicellulose, followed by a third mass loss of about 12.61% corresponding to the decomposition of cellulose. The last weight loss of 5.88% was due to the decomposition lignin [31].

3.1.4. SEM/EDX analysis

The SEM images of Clay, Biochar and composite are shown in Figure 3. The surface of CL was smooth with many hollow surfaces as can be observed in Figure 3a. BC sample a porous structure, and exhibited an uneven and rough surface (Figure 3b). For CBC (Figure 3c), CL particles were deposited on the surface of BC but the surface was not entirely covered by the clay [18, 32].

The chemical composition of the adsorbents was investigated by the EDX analysis. EDX spectra of clay in Figure 3a presented high peaks of the

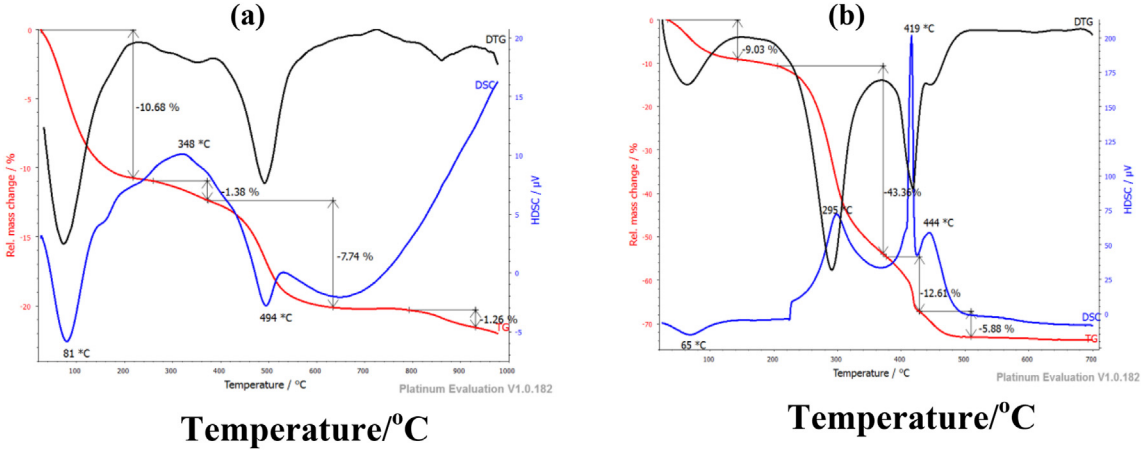

Figure 2. TG, DTG and DSC spectra of a) raw Clay and (b) cotton wood.

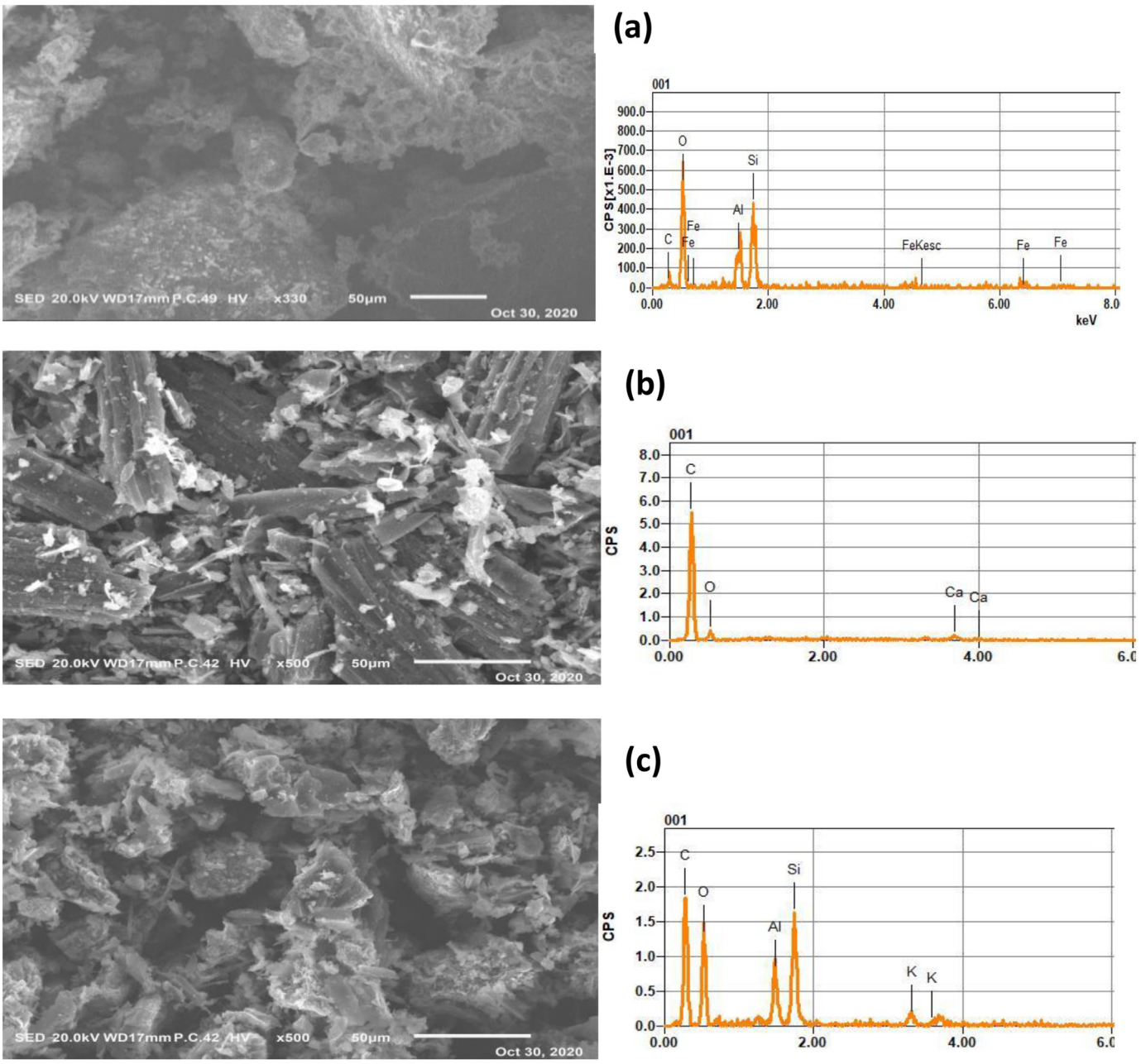

Figure 3. SEM images coupled with EDX composition analysis of (a) CL, (b) BC and (c) CBC.

constituent elements silicon, aluminium, oxygen, and iron which are mainly elemental composition of clay. Nevertheless, the constituent elements observed in biochar were carbon, oxygen and calcium. Whereas, the EDX spectra of composite (Figure 3c) compared with other spectra (Figure 3a,b) provided evidence for the existence of clay on the surface of biochar.

3.2. Sorption studies

3.2.1. Influence of contact time

The adsorption kinetics of glyphosate on clay, biochar, and composite were evaluated using the same initial fixed glyphosate concentration (50 mg L^{-1}) with contact times varying between 5 and 240 mn at pH (6.5) as shown in Figure 5a. It can be observed that the adsorption of glyphosate by CL and the CBC were reached equilibrium after 2 h while for BC the adsorption was reached equilibrium after 1 h. The glyphosate adsorption was found higher with the CBC than both CL and BC. This may be due to the high mineral content, high electrical conductivity in clay and the great capacity of ionic exchange of biochar.

Table 1. Kinetic parameters for glyphosate absorption.

Kinetic model	Adsorbent	Parameters		
		q_e (mg/g)	k_1 (min^{-1})	R^2
Pseudo-first-order model	CL	4.160	0.028	0.988
	BC	22.540	0.058	0.923
	CBC	24.749	0.025	0.987
		q_e (mg/g)	**k_2 (g/mg/min)**	R^2
Pseudo-second-order model	CL	4.966	0.008	0.996
	BC	20.877	0.004	0.995
	CBC	41.010	0.002	0.999

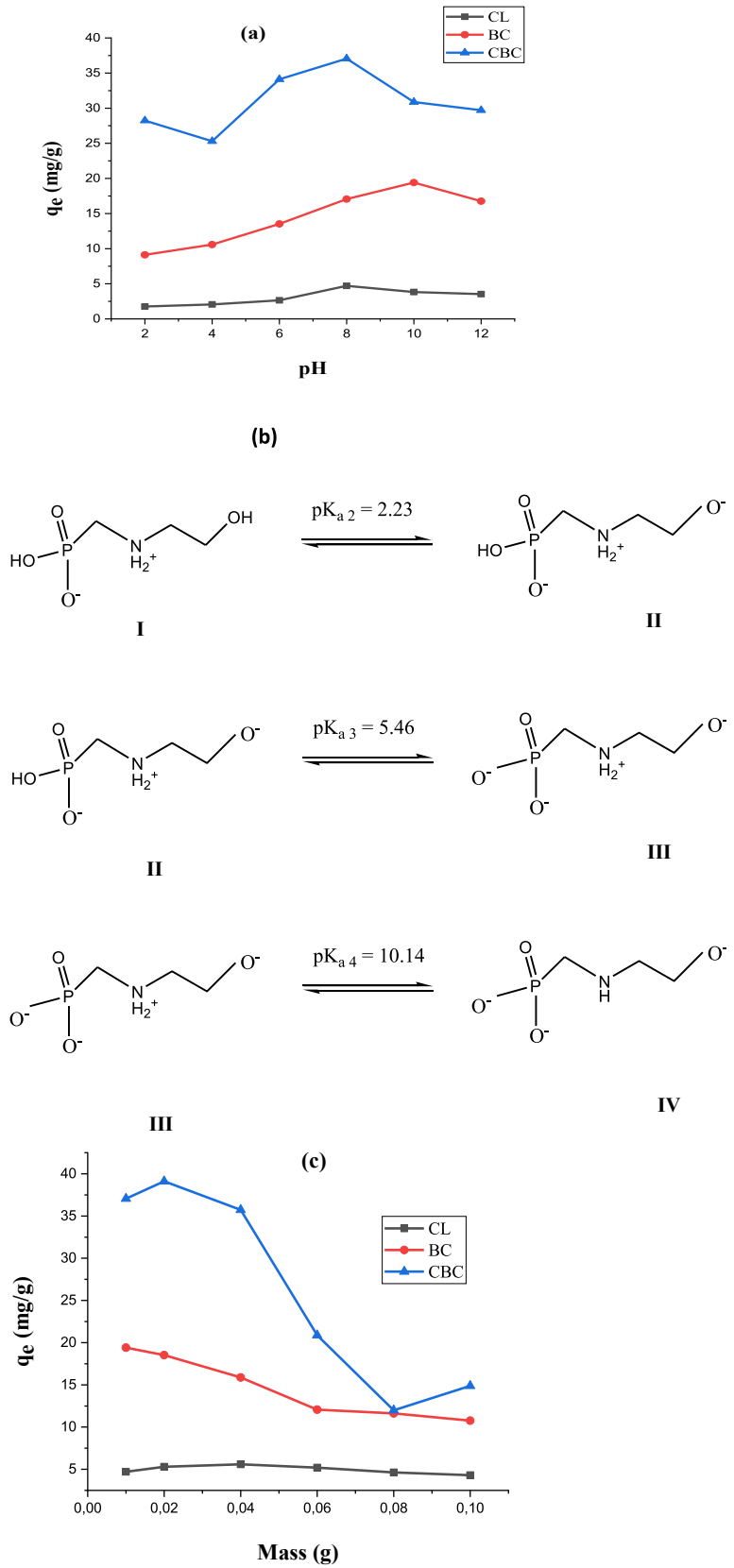

Figure 4. (a) Effect of pH on the adsorption of glyphosate (10 mg of adsorbent; 50 mL of solution containing 50 mg L^{-1} of glyphosate; 2 h of contact time; 25 °C) (b) Glyphosate acid-base equilibrium (I, II, III, IV = Ionic states of glyphosate as a function of pH) [34] (c) Effect of the adsorbent dose on glyphosate removal (50 mL of solution containing 50 mg L^{-1} of glyphosate; 2 h of contact time; pH 6.5; 25 °C).

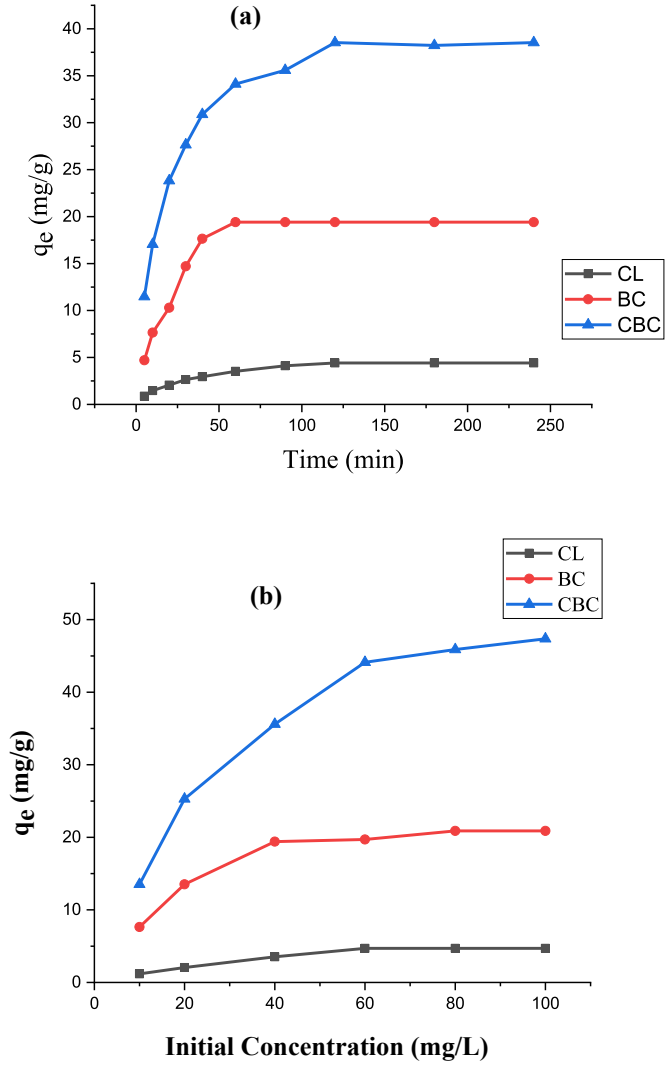

Figure 5. (a) Effect of contact time, (b) initial concentration on the adsorption of glyphosate by different adsorbents.

Parameters of the pseudo-first order kinetic and the pseudo-second order kinetic are summarized in Table 1. The R^2 of pseudo-second kinetic are 0.996, 0.995, 0.999 while the R^2 of pseudo-first kinetic are 0.988, 0.923, 0.987 respectively for CL, BC and CBC. The R^2 of pseudo-second order showed higher values compared with the R^2 of pseudo-first order and the calculated adsorption capacities of pseudo-second order are similar to the experimental adsorption capacities, thereby indicating that chemisorption plays a major role in the process of adsorption [33].

3.2.2. *Influence of pH*

The pH is an important parameter affecting the adsorption of the glyphosate in aqueous solution depending on the state of materials. Maximum removal of 4.71, 19.41 and 37.06 mg/g were obtained at pH 8, 10 and 8 for CL, BC and CBC respectively. As shown in Figure 4a. The adsorption efficiencies of glyphosate increased slowly with pH in the case of Clay and Biochar, and decreased after pH 8 for clay and pH 10 for Biochar. Meanwhile the adsorption capacity of glyphosate for the composite sample decreased from pH 2 to 4. This was followed by an increase to a maximum at pH 8. Glyphosate exhibits different functional groups in solution at different pH (Figure 4b) [34]. The constant and the equilibrium reactions of acid-base dissociation of glyphosate are shown in Figure 4b. At lower pH the species I and II should be dominant in solution. But as pH goes more basic (weaker acid), the species III and IV become more dominant and enhanced adsorption as they possess more active sites for binding on adsorbent. This more evident with species **IV** (NH^{2+} →NH), suggesting enhanced adsorption at pH 8 was due to this glyphosate species. Hence, the adsorption process could be occurring by surface complex formation via the three phosphonate groups and NH coordination to the adsorbents surfaces [34].

Table 2. Langmuir, Freundlich and Temkin parameters on the adsorption of glyphosate.

Model	Adsorbent	Isotherm parameters		
Langmuir		**q_{max} (mg/g)**	**k_L (L/mg)**	**R^2**
	CL	0.159	46.154	0.937
	BC	1.685	14.631	0.989
	CBC	2.712	22.148	0.993
Freundlich		**n**	**k_F (mg/g) (L/mg)$^{1/n}$**	**R^2**
	CL	2.045	5.913	0.928
	BC	2.490	3.814	0.850
	CBC	2.045	5.913	0.928
Temkin		**b (J/mol)**	**k_T (L/g)**	**R^2**
	CL	13.812	0.396	0.982
	BC	13.812	0.818	0.909
	CBC	13.812	0.396	0.983

3.2.3. *Influence of adsorbent dose*

As shown in Figure 4c, the glyphosate equilibrium adsorption capacities decreased with increasing BC and CBC dose. The BC and CBC displayed excellent adsorption capacities at low dose. This result might be due to overcrowding of active sites of the adsorbents as well as specific surface area which may reduce the adsorption capacities. As for CL, the increase of adsorbent dose up to a maximum of 0.04 g increased adsorption capacity of glyphosate, followed by a decrease at 0.06 g. This Increase in adsorption might be due to the increase in surface area, and hence the number of active sites [18].

3.2.4. *Influence of initial concentration*

The Figure 5b showed the adsorption of glyphosate on clay, biochar, and composite at different initial concentrations. The equilibrium adsorption amount of glyphosate increased quickly at low concentration. Then, the adsorption capacity increased slowly and reached stabilization at last. As seen in this figure, the CBC showed the best performances in the adsorption of glyphosate than BC and CL.

Three adsorption isotherms models of Langmuir, Freundlich and Temkin were fitted and their characteristics where presented in Table 2. Calculated values of correlation coefficient R^2, shows that Langmuir model best fitted glyphosate adsorption on Biochar and Clay-Biochar composite whereas Temkin model fitted adsorption on Clay. Therefore, the Langmuir isotherm indicated that all adsorbents had homogeneous surfaces made up of monolayer [6]. The fitting of Temkin isotherm suggest that the adsorption of glyphosate was controlled by electrostatic interaction of chemical adsorption.

4. Conclusion

The clay-biochar composite made from Clay and cotton wood by pyrolysis in this present study was performed successfully with improved properties as clearly shown by the presence of clay on the surface of biochar. Batch system was investigated to perform the adsorption of glyphosate on Clay, Biochar and Clay-Biochar composite. The sorption process was analyzed through operating conditions such as contact time, pH, adsorbent dose and initiale concentration. The Clay-Biochar composite showed significantly high glyphosate adsorption capacity than the original Clay and Biochar. Pseudo-second order kinetics model showed best fit of glyphosate adsorption on the three samples. The Langmuir and Temkin model were more suitable for describing the equilibrium adsorption data for all the adsorbents. Thus, clay-biochar composite can

be used for the removal of glyphosate containing waste water. The effect of different clay/biochar ratio on glyphosate adsorption should be further studied to improve the removal process.

Declarations

Author contribution statement

Danga Rallet: Performed the experiments; Analyzed and interpreted the data; Wrote the paper.

Abba Paltahe, Cornelius Tsamo: Conceived and designed the experiments; Analyzed and interpreted the data; Contributed reagents, materials, analysis tools or data.

Benoît Loura: Analyzed and interpreted the data; Contributed reagents, materials, analysis tools or data.

Funding statement

This research did not receive any specific grant from funding agencies in the public, commercial, or not-for-profit sectors.

Data availability statement

Data will be made available on request.

Declaration of interests statement

The authors declare no conflict of interest.

Additional information

No additional information is available for this paper.

References

[1] S. Varjani, G. Kumar, E.R. Rene, Developments in biochar application for pesticide remediation: current knowledge and future research directions, J. Environ. Manag. 232 (2019).
[2] Abhishek Mandal, Neera Singh, Optimization of atrazine and imidacloprid removal from water using biochars: designing single or multi-staged batch adsorption systems, Int. J. Hyg Environ. Health 220 (2017).
[3] F. Maggi, D. la Cecilia, F.H.M. Tang, A. McBratney, The global environmental hazard of glyphosate use, Sci. Total Environ. 717 (2020).
[4] L. Caceres-Jensen, J. Rodríguez-Becerra, P. Sierra-Rosales, Electrochemical method to study the environmental behavior of Glyphosate on volcanic soils: Proposal of adsorption-desorption and transport mechanisms, J. Hazard Mater. 379 (2019).
[5] F.M. Flores, R.M.T. Sánchez, M.d.S. Afonso, Some aspects of the adsorption of glyphosate and its degradation products on montmorillonite, Environ. Sci. Pollut. Contr. Ser. 25 (2018).
[6] C. Tsamo, M. Assabe, J. Argue, S.O. Ihimbru, Discoloration of methylene blue and slaughter house wastewater using maize cob biochar produced using a constructed burning chamber: a comparative study, Sci. Afr. 3 (2019).
[7] S. Ismadji, D.S. Tong, F.E. Soetaredjo, A. Ayucitra, W.H. Yu, C.H. Zhou, Reprint of Bentonite hydrochar composite for removal of ammonium from Koi fish tank, Appl. Clay Sci. 119 (2015).
[8] E. Viglašová, M. Galamboš, Z. Danková, L. Krivosudský, C.L. Lengauer, R. Hood-Nowotny, G. Soja, A. Rompel, Ma. Matík, J. Briančin, Production, characterization and adsorption studies of bamboo-based biochar/montmorillonite composite for nitrate removal, Waste Manag. 79 (2018).
[9] P. Djomgoue, D. Njopwouo, FT-IR spectroscopy applied for surface clays characterization, J. Surf. Eng. Mater. Adv. Technol. 3 (2013).
[10] A. Shaaban, S. Se, N.M.M. Mitan, M.F. Dimin, Characterization of biochar derived from rubber wood sawdust through slow pyrolysis on surface porosities and functional groups, Procedia Eng. 68 (2013).
[11] A.U. Rajapaksha, S.S. Chen, D.C.W. Tsang, M. Zhang, M. Vithanage, S. Mandal, B. Gao, N.S. Bolan, Y.S. Ok, Engineered/designer biochar for contaminant removal/immobilization from soil and water: potential and implication of biochar modification, Chemosphere 148 (2016).
[12] M.A. Franciski, E.C. Peres, M. Godinho, D. Perondi, E.L. Foletto, G.C. Collazzo, G.L. Dotto, Development of CO2 activated biochar from solid wastes of a beer industry and its application for methylene blue adsorption, Waste Manag. 78 (2018).
[13] D.A.G. Sumalinog, S.C. Capareda, M.D.G. de Luna, Evaluation of the effectiveness and mechanisms of acetaminophen and methylene blue dye adsorption on activated biochar derived from municipal solid wastes, J. Environ. Manag. 210 (2018).
[14] G. Yang, L. Wu, Q. Xian, F. Shen, J. Wu, Y. Zhang, Removal of Congo red and methylene blue from aqueous solutions by vermicompost-derived biochars, PLoS One 11 (2016).
[15] L. Meili, P.V. Lins, C.L.P.S. Zanta, J.I. Soletti, L.M.O. Ribeiro, C.B. Dornelas, T.L. Silva, M.G.A. Vieira, sMgAl-LDH/Biochar composites for methylene blue removal by adsorption, Appl. Clay Sci. 168 (2019).
[16] C. Trigo, L. Cox, K. Spokas, Influence of pyrolysis temperature and hardwood species on resulting biochar properties and their effect on azimsulfuron sorption as compared to other sorbents, Sci. Total Environ. 566 (2016).
[17] X. Wang, Y. Gu, X. Tan, Y. Liu, Y. Zhou, X. Hu, X. Cai, W. Xu, C. Zhang, S. Liu, Functionalized biochar/clay composites for reducing the bioavailable fraction of arsenic and cadmium in river sediment, Environ. Toxicol. Chem. 38 (2019).
[18] K.S.D. Premarathna, A.U. Rajapaksha, N. Adassoriya, B. Sarkar, N.M.S. Sirimuthu, A. Cooray, Y.S. Ok, M. Vithanage, Clay-biochar composites for sorptive removal of tetracycline antibiotic in aqueous media, J. Environ. Manag. 238 (2019).
[19] Y. Yao, B. Gao, J. Fang, M. Zhang, H. Chen, Y. Zhou, A.E. Creamer, Y. Sun, L. Yang, Characterization and environmental applications of clay–biochar composites, Chem. Eng. J. 242 (2014).
[20] H.Z. Adjia1, F. Villiéras, R. Kamga1, F. Thomas, Mineralogy and physico-chemical properties of alluvial clays from far-north region of Cameroon: a tool for an environmental problem, Int. J. Water Resour. Environ. Eng. 5 (2013).
[21] Y.S. Hua, Y.Q. Zhaoa, B. Sorohan, Removal of glyphosate from aqueous environment by adsorption using water industrial residual, Desalination 271 (2011).
[22] A. Kumar, P. Lingfa, Sodium bentonite and kaolin clays: comparative study on their FT-IR, XRF, and XRD, Mater. Today: Proc. 22 (2019).
[23] A. Mbaye, C.A.K. Diop, M.B. Jocelyne, F. Senocq, F. Maury, Characterization of natural and chemically modified kaolinite from Mako (Senegal) to remove lead from aqueous solutions, Clay Miner. 49 (2014).
[24] R. Dewi, H. Agusnar, Z. Alfian, Tamrin, Characterization of technical kaolin using XRF, SEM, XRD, FTIR and its potentials as industrial raw materials, J. Phys. Conf. 1116 (2018).
[25] O. Ngomo, J.M. Sieliechi, J.B. Tchatchueng, R. Kamga, A. Tabacaru, R. Dinica, M. Praisler, Differences between structural, textural and rheological properties of two Cameroonian mineral clays used as cosmetic mask, Adv. Environ. Sci. Develop. Chem. (2014) 19–21.
[26] V.H. Gomdje, G.P. Kofa, A. Wahabou, B. Loura, A. Chtaini, B. Subramanian, Synthesis of Polyvinylpyrrolidone-natural swelling clay composites: application for complexation of Pb2+, Arab J. Phys. Chem. (2017).
[27] Q. Yin, H. Ren, R. Wang, Z. Zhao, Evaluation of nitrate and phosphate adsorption on Al-modified biochar: influence of Al content, Sci. Total Environ. 631 (2018).
[28] S. Liu, J. Li, S. Xu, M. Wang, Y. Zhang, X. Xue, A modified method for enhancing adsorption capability of banana pseudostem biochar towards methylene blue at low temperature, Bioresour. Technol. 282 (2019).
[29] E. Tiffo, A. Elimbi, J.D. Manga, A.B. Tchamba, Red ceramics produced from mixtures of kaolinite clay and waste glass, Brazil. J. Sci. Technol. 2 (2015).
[30] H. Abdulrazzaq, H. Jol, A. Husni, R. Abu-Bakr, Characterization and stabilisation of biochars obtained from empty fruit bunch, wood, and rice husk, Bioresources 9 (2) (2014).
[31] J.H.F. de Jesus, G. da C. Cunha, E.M.C. Cardoso, A.S. Mangrich, L.P.C. Romeao, Evaluation of waste biomasses and their biochars for removal of polycyclic aromatic hydrocarbons, J. Environ. Manag. 200 (2017).
[32] L. Chen, X.L. Chen, C.H. Zhou, H.M. Yang, S.F. Ji, D.S. Tong, Z.K. Zhong, W.H. Yu, M.Q. Chu, Environmental-friendly montmorillonite-biochar composites: facile production and tunable adsorption-release of ammonium and phosphate, J. Clean. Prod. 156 (2017).
[33] Z. Labaali, S. Kholtei, J. Naja, Co^{2+} removing from wastewater using apatite preparedthrough phosphate waste rock valorisation: equilibrium, kinetic and thermodynamics stadies, Sci. Afr. 8 (2020).
[34] R. Tévez, M. Afonso, pH dependence of Glyphosate adsorption on soil horizons, Bol. Soc. Geol. Mex. 67 (3) (2015) 509–516.